Journal of Dermatological Science 94 (2019) 346–349

Contents lists available at ScienceDirect

Journal of Dermatological Science

journal homepage: www.jdsjournal.com

Letter to the Editor

3D *in vivo* imaging of the keratin filament network in the mouse stratum granulosum reveals profilaggrin-dependent regulation of keratin bundling

Keratins are epithelium-specific intermediate filaments ~10 nm in diameter. Sequential expression of type I and II keratin genes correlates with epidermal differentiation [1]. Keratin 5 and 14 are first expressed in the stratum basale (SB). In the stratum spinosum (SS), keratin 1 and 10 begin to be expressed. In the stratum granulosum (SG), some keratins form amorphous aggregates called keratohyalin granules (KHGs) [2]. Filaggrin (*Flg*) is first expressed as profilaggrin and localizes to KHGs in the SG layers [3]. During cornification, profilaggrin linker peptides are cleaved, releasing monomer filaggrin, which bundles keratin filaments in the lower stratum corneum (SC) to form highly dense keratin filament networks, contributing to SC mechanical strength [4–6]. Mutations in human *FLG* are a major predisposing factor for atopic dermatitis [7], and filaggrin-deficient ($Flg^{-/-}$) mice exhibit aberrant SC barrier function, possibly due to the irregularly arranged keratin filaments in SC [8]. Therefore, it is assumed that the filaggrin–keratin interaction in SC affects SC barrier function, though its role in SG cells is unclear. The purpose of this study was to visualize keratin filament networks in living SG cells and reveal the contribution of profilaggrin expression to the keratin network in SG cells of live mice.

Intracellular localization of exogenously expressed fluorescent fusion protein, mCherry-keratin 1 (mCherry-K1), was examined in living and fixed HeLa cells by immunofluorescent staining and in primary cultured keratinocytes by correlative light and electron microscopy (CLEM) (Fig. S1a–c). Exogenously expressed mCherry-K1 labeled bundled keratin filaments in both HeLa cells and mouse primary cultured keratinocytes without disturbing endogenous keratin networks. Immunoblotting confirmed that full-length mCherry-K1 was expressed in both cells (Fig. S1d and e).

To express mCherry-K1 transiently and sporadically *in vivo*, we intradermally injected a plasmid encoding mCherry-K1 under control of the CMV promoter (pmCherry-K1), followed by *in vivo* electroporation into the back skin of hairless H2B-EGFP mice, the nuclei of which were labeled by ubiquitous expression of EGFP fused with histone 2B [9]. mCherry-K1 preferentially expressed in SG cells formed clear mesh-like bundled keratin networks in the cytoplasm and was not incorporated into round KHG-like material, recognized by the absence of mCherry-K1 signal in the SG cell cytoplasm (Fig. 1a, arrowheads and Movie 1). Highly bundled keratin filaments were arranged along the edges of polygonal SG cells (Fig. 1a, arrows), indicating that mCherry-K1 expression enabled visualization of the cytoplasmic keratin network of SG cells in live mice.

To analyze the effect of filaggrin deficiency, pmCherry-K1 plasmid was electroporated into the back skin of $Flg^{+/+}$ or $Flg^{-/-}$ hairless mice. Immunoblotting analysis confirmed that full-length mCherry-K1 protein was expressed in electroporated epidermis (Fig. S2). The mCherry-K1 signals of $Flg^{-/-}$ SG cells revealed diffuse and ambiguous keratin filament, whereas $Flg^{+/+}$ mice showed robust and parallel keratin networks (Fig. 1b). The mCherry-K1 signals of heterozygous $Flg^{+/-}$ SG cells did not differ from those of $Flg^{+/+}$ SG cells, and expression of keratin 5/14 and keratin 1/10 mRNAs was normal in $Flg^{-/-}$ epidermis (data not shown). Round KHG-like material was not apparent in $Flg^{-/-}$ SG cells (Fig. 1a). To quantitatively analyze mCherry-K1 filament networks, we derived line profiles of fluorescence intensity in the selected SG cells (Fig. 1c). The mCherry-K1 line profiles of $Flg^{-/-}$ SG cells were clearly distinguishable from those of $Flg^{+/+}$ cells, with the former having a shorter periodic structure with smaller signal amplitude (Fig. 1c, left). These line profiles, representing the relationship between the periodic length of the structure and its fluorescent intensity (*i.e.* power), were then confirmed by subjecting $Flg^{+/+}$ and $Flg^{-/-}$ SG cells to Fourier transform. Resulting power spectra of $Flg^{+/+}$ SG cells exhibited intense signals from the large periodic structures (typically >1 μm), while most of the fluorescent intensity of $Flg^{-/-}$ cells was attributed to structures <1 μm (Fig. 1d, right). The decreased number of bundled keratin filaments was also demonstrated by principal component analysis (PCA), which included 38–39 line profiles each from $Flg^{+/+}$ (N = 9) and $Flg^{-/-}$ (N = 11) SG cells. The scatter plot (Fig. 1d) shows that the mCherry-K1 signals from $Flg^{+/+}$ and $Flg^{-/-}$ SG cells are statistically different. The higher absolute values of $Flg^{-/-}$ cells on the PC22 axis points to the shorter periodic lengths of the keratin structures that were more abundant in $Flg^{-/-}$ SG cells.

To confirm the abnormality of overall keratin filaments in $Flg^{-/-}$ SG cells by EM, we first confirmed that most of the mCherry-K1 filament networks in living SG cells did not change after chemical fixation (Fig. S3a). Vertical sections of $Flg^{+/+}$ and $Flg^{-/-}$ epidermis revealed that KHGs were observed *via* EM as round, electron-dense granules surrounded by irregularly-shaped pale material (Fig. 2a). In contrast, these KHGs were hardly observed in $Flg^{-/-}$-SG cells. Instead, stellate irregularly shaped KHGs were formed. However, the overall keratin network could not be observed in vertical section images. To observe the cytoplasmic distribution of keratin filaments more clearly, we used horizontal sections of mouse epidermis (Fig. S3b, Fig. 2b). Horizontal sections revealed bundled endogenous keratin networks of $Flg^{-/-}$ SG cells showing significantly fewer bundled keratin networks compared to that in $Flg^{+/+}$ SG cells (Fig. 2b and d). In contrast, the areas of the bundled keratin filaments in SS cells were not significantly different between $Flg^{+/+}$ and $Flg^{-/-}$ mice (Fig. 2b and c). These results suggested that SG cells exhibit keratin-bundling mechanisms different from those of SB and SS cells. Although most profilaggrin is thought to localize in the

https://doi.org/10.1016/j.jdermsci.2019.04.006

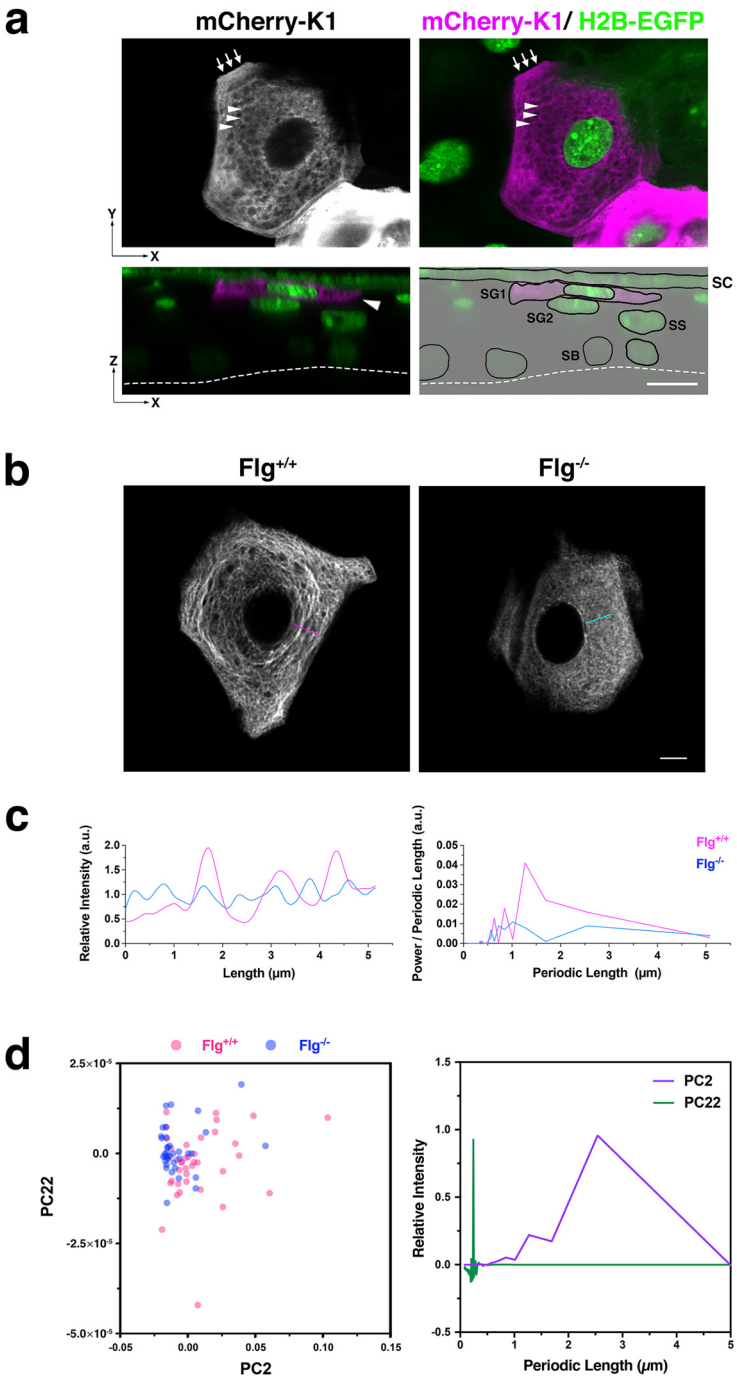

Fig. 1. Intravital visualization of mCherry-K1 expressed in a single SG cell and aberrant keratin filament networks in *Flg*$^{-/-}$ SG cells.
(a) (Upper panels) Representative *in vivo* confocal microscopic images of sporadically expressed mCherry-K1 in the upper epidermis of the back skin of a H2B-EGFP-expressing hairless mouse by electroporation. The pmCherry-K1 plasmid was intradermally injected into the back skin of an H2B-EGFP-expressing hairless mouse (5-week-old, male). After 42 h, the mouse was anesthetized and observed by confocal microscopy. Expressed mCherry-K1 signals (*mCherry-K1*; white in left panel and magenta in right panel) in SG cells showed keratin filament networks in the cytoplasm. Keratin networks were bundled at the edge (arrows) and cytoplasm (arrowheads) and localized between round KHGs (approximately >1–2 μm in diameter), which were recognized by the absence of mCherry-K1 signal. H2B-EGFP (green) indicated the position of the nucleus.
(Lower panels) A reconstructed vertical image of z-axis scanning confocal images (left panel) indicated that mCherry-K1 was expressed in the SG1 cell layer (arrowhead) based on the nuclear location. The scheme for the reconstructed vertical image of the mouse epidermis is shown in the right panel. SC layer, nuclear positions of SG1, SG2, SS, and SB are indicated according to the signals of H2B-EGFP. Identification of SG3 was difficult in this image. Dashed lines represent the border between the epidermis and dermis. Scale bar: 10 μm.
(b) Representative *in vivo* confocal microscopic images of SG cells sporadically expressing mCherry-K1 in *Flg*$^{+/+}$ and *Flg*$^{-/-}$ hairless mice by electroporation. The back skin of *Flg*$^{+/+}$ and *Flg*$^{-/-}$ adult hairless mice was electroporated with pmCherry-K1. After 53 h, the mice were anesthetized and observed by confocal microscopy. Note the ambiguous and diffuse keratin filament network in *Flg*$^{-/-}$ mice. Lines indicate the position of line profiles of fluorescence intensity in (c). Scale bar: 5 μm.
(c) Line profiles of mCherry-K1 fluorescent intensity in *Flg*$^{+/+}$ (magenta) and *Flg*$^{-/-}$ (blue) mice plotted from the colored lines in (b) (left). Power spectra against wave number, calculated from the Fourier transform of each line profile (right). mCherry-K1 power spectra of *Flg*$^{-/-}$ SG cells are characterized as a short periodic length.
(d) Principal component analysis of power spectra in (c). Scatter plots of PC2 *versus* PC22 data of mCherry-K1 signals in *Flg*$^{+/+}$ (magenta circles; N = 38 from 9 cells) and *Flg*$^{-/-}$ (blue circles; N = 39 from 11 cells) SG cells (left). mCherry-K1 signals in *Flg*$^{+/+}$ SG cells were significantly different from those in *Flg*$^{-/-}$ SG cells in both PC2 ($p < 0.05$) and PC22 ($p < 0.05$) (Student's *t*-test). Graphs of coefficients for PC2 (coefficient; 2.54 μm) and PC22 (coefficient; 0.24 μm) are also shown (right).

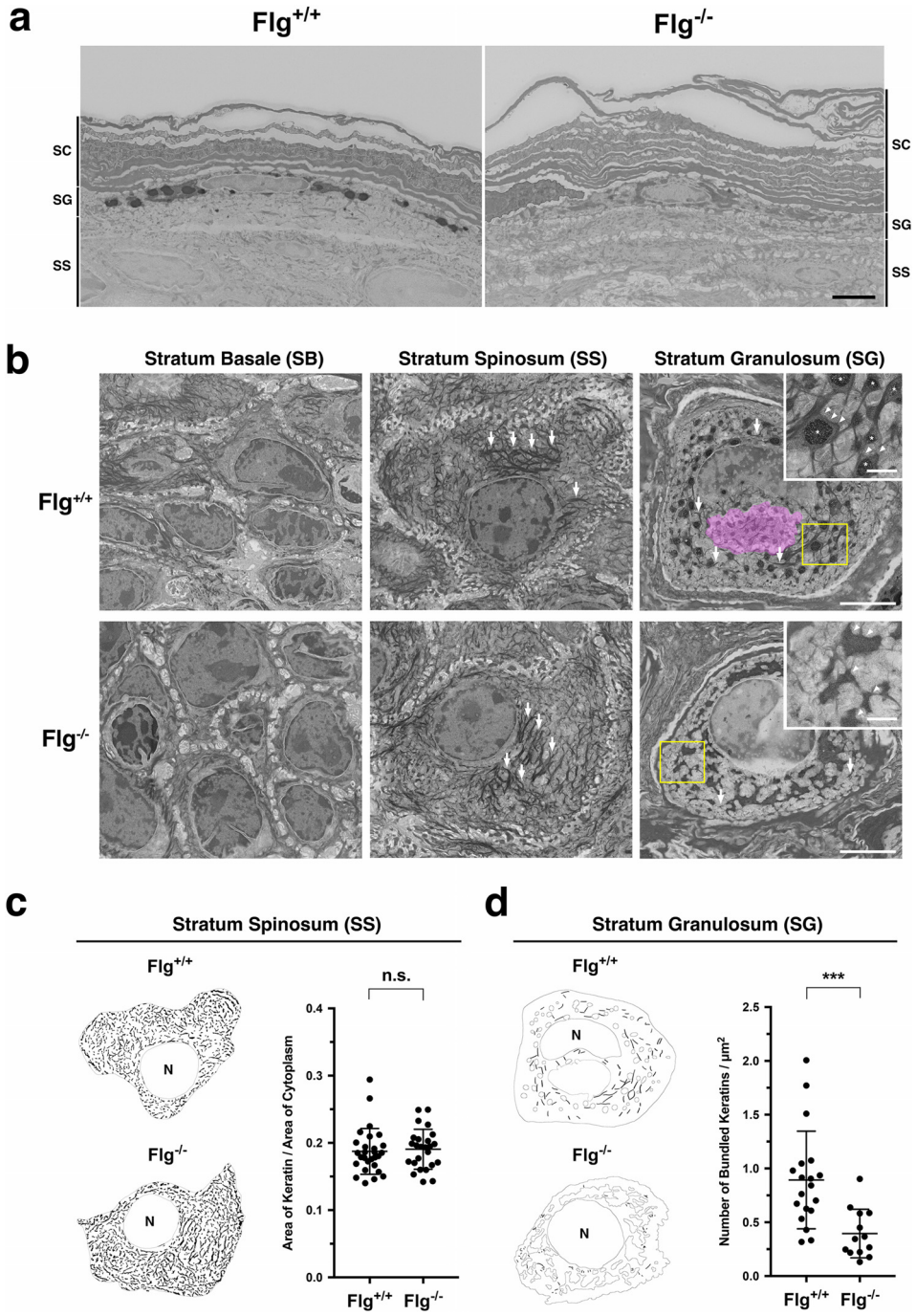

Fig. 2. Aberrant KHGs and reduced bundled keratin filament networks in fixed *Flg*$^{-/-}$ SG cells revealed by EM analysis.
(a) Representative field emission-scanning electron microscopy images of vertical sections of isolated epidermis from the back skin of *Flg*$^{+/+}$ and *Flg*$^{-/-}$ hairless mice. Stratum spinosum (*SS*), stratum granulosum (*SG*), and stratum corneum (*SC*) are indicated. Scale bar: 30 μm.
(b) Representative images of horizontal sections of (a) stratum basale (*SB*), SS, and SG of *Flg*$^{+/+}$ (upper panels) or *Flg*$^{-/-}$ (lower panels) epidermis. The adjacent cell is shown in magenta in the image of the *Flg*$^{+/+}$ SG cell. Bundled keratin filaments in SS and SG cells are indicated by arrowheads. The yellow boxed areas are enlarged in each of the panel insets. Asterisks indicate electron-dense round KHGs surrounded by irregularly shaped KHGs (arrowhead) in *Flg*$^{+/+}$ SG cells. Irregularly shaped KHG-like material (arrowhead) was also found in *Flg*$^{-/-}$ SG cells. Scale bar: 5 μm and 1 μm (insets).
(c) Area of bundled keratin filaments per cell area of *Flg*$^{+/+}$ or *Flg*$^{-/-}$ SS cells in (b) was analyzed using ImageJ (left images, nucleus [*N*]). *Flg*$^{+/+}$ (N = 28 cells) and *Flg*$^{-/-}$ (N = 25 cells) SS cells were analyzed and showed indistinguishable areas of bundled keratin filaments per cell area (right graph).
(d) The number of bundled keratin filaments (>0.09 μm in diameter) in original SG images (shown in b) traced manually (shown in thick black lines) were counted and divided by the cytoplasmic area excluding the KHG area (left images, nucleus (*N*)). The number of bundled keratin filaments in SG cells was significantly decreased in *Flg*$^{-/-}$ mice (N = 13 cells) compared to that in *Flg*$^{+/+}$ mice (N = 19 cells) (***$p < 0.05$, Student's *t*-test).

KHGs of SG cells, it is also possible that some profilaggrin is cleaved into filaggrin in the SG layers and involved directly or indirectly in keratin bundling. In *Flg* mutation carriers in humans, truncated profilaggrin can be produced from mutant *Flg* alleles [3]. In the future, the rescue of full-length or truncated profilaggrin expression in SG cells of *Flg*$^{-/-}$ mice may be useful in determining which part of profilaggrin is responsible for keratin bundling in SG cells. Therefore, the visualization of the keratin filament network in SG

cells *in vivo* enables dissection of the regulation of the keratin network, which is important for understanding the function of SC.

Funding

This study was supported in part by a JSPS Grant-in-Aid for Scientific Research (C) under Grant Number JP25461667 to T. Matsui, AMED under Grant Number JP18gm1010001 to M. Amagai and T. Matsui, and the Takeda Science Foundation to T. Matsui. This work was supported by RIKEN Junior Research Associate Program and a Nagai Memorial Research Scholarship from the Pharmaceutical Society of Japan to K. Usui.

Disclosure

The authors have no conflict of interest to declare.

Acknowledgements

We thank all members of our laboratory, especially, Rika Yokoo, Ritsuko Ozawa, and Sachie Marushima for technical assistance, and Hachiro Iseki and Dr. Ai Hirabayashi for EM analysis. We also thank Dr. Takaharu Okada for live imaging, Ryosuke Yamazaki for image analysis, and Dr. Hiroyuki Sasaki for critical reading of manuscript. We also thank JKiC (JSR-Keio University Medical and Chemical Innovation Center) for special assistance for imaging analysis.

Appendix A. Supplementary data

Supplementary material related to this article can be found, in the online version, at doi:https://doi.org/10.1016/j.jdermsci.2019.04.006.

References

[1] J.T. Jacob, P.A. Coulombe, R. Kwan, M.B. Omary, Types I and II keratin intermediate filaments, Cold Spring Harb. Perspect. Biol. 10 (2018)a018275.
[2] K.A. Holbrook, Biologic structure and function: perspectives on morphologic approaches to the study of the granular layer keratinocyte, J. Invest. Dermatol. 92 (1989) 84–104.
[3] A. Sandilands, C. Sutherland, A.D. Irvine, W.H. McLean, Filaggrin in the frontline: role in skin barrier function and disease, J. Cell Sci. 122 (2009) 1285–1294.
[4] T. Matsui, M. Amagai, Dissecting the formation, structure and barrier function of the stratum corneum, Int. Immunol. 27 (2015) 269–280.
[5] B.B.A. Dale, K.A. Holbrook, P.M. Steinert, Assembly of stratum-corneum basic-protein and keratin filaments in macrofibrils, Nature 276 (1978) 729–731.
[6] L. Norlen, S. Masich, K.N. Goldie, A. Hoenger, Structural analysis of vimentin and keratin intermediate filaments by cryo-electron tomography, Exp. Cell Res. 313 (2007) 2217–2227.
[7] C.N. Palmer, A.D. Irvine, A. Terron-Kwiatkowski, Y. Zhao, H. Liao, S.P. Lee, D. R. Goudie, A. Sandilands, L.E. Campbell, F.J. Smith, G.M. O'Regan, R.M. Watson, J.E. Cecil, S.J. Bale, J.G. Compton, J.J. DiGiovanna, P. Fleckman, S. Lewis-Jones, G. Arseculeratne, A. Sergeant, C.S. Munro, B. El Houate, K. McElreavey, L.B. Halkjaer, H. Bisgaard, S. Mukhopadhyay, W.H. McLean, Common loss-of-function variants of the epidermal barrier protein filaggrin are a major predisposing factor for atopic dermatitis, Nat. Genet. 38 (2006) 441–446.
[8] H. Kawasaki, K. Nagao, A. Kubo, T. Hata, A. Shimizu, H. Mizuno, T. Yamada, M. Amagai, Altered stratum corneum barrier and enhanced percutaneous immune responses in filaggrin-null mice, J. Allergy Clin. Immunol. 129 (2012) 1538–1546.e6.
[9] T. Abe, H. Kiyonari, G. Shioi, K. Inoue, K. Nakao, S. Aizawa, T. Fujimori, Establishment of conditional reporter mouse lines at ROSA26 locus for live cell imaging, Genesis 49 (2011) 579–590.

Keiko Usui[a,b], Nanako Kadono[a,c], Yuki Furuichi[a,d], Keiichiro Shiraga[a], Takashi Saitou[e], Hiroshi Kawasaki[d,f], Kiminori Toyooka[g], Hiroomi Tamura[b], Akiharu Kubo[d], Masayuki Amagai[a,d], Takeshi Matsui[a,*]

[a]Laboratory for Skin Homeostasis, RIKEN Center for Integrative Medical Sciences, Yokohama, Japan
[b]Department of Hygienic Chemistry, Faculty of Pharmacy, Keio University, Tokyo, Japan
[c]KOSÉ Endowed Course for Skin Care and Allergy Prevention II, The Department of Dermatology, Keio University School of Medicine, Tokyo, Japan
[d]Department of Dermatology, Keio University School of Medicine, Tokyo, Japan
[e]Translational Research Center, Ehime University Hospital, Toon, Japan
[f]Disease Biology Group, RIKEN Medical Sciences Innovation Hub Program, Yokohama, Japan
[g]Mass Spectrometry and Microscopy Unit, RIKEN Center for Sustainable Resource Science, Yokohama, Japan

* Corresponding author at: Laboratory for Skin Homeostasis, RIKEN Center for Integrative Medical Sciences (IMS), 1-7-22, Suehirocho, Tsurumi-ku, Yokohama, Kanagawa, 230-0045, Japan.
E-mail address: takeshi.matsui@riken.jp (T. Matsui).

Received 25 December 2018
Received in revised form 24 April 2019
Accepted 26 April 2019